Electric-field-driven nano-oxidation trimming of silicon microrings and interferometers

Yiran Shen,[1,*] Ivan B. Divliansky,[2] Dimitri N. Basov,[1] and Shayan Mookherjea[1]

[1]*University of California, San Diego, Mail Code 0407, La Jolla, California 92093, USA*

[2]*College of Optics and Photonics (CREOL), University of Central Florida, Orlando, Florida 32816-2700, USA*

Corresponding author: yis004@ucsd.edu

Nanoscale disorder results in severe spectral misalignment of silicon microring resonators and Mach–Zehnder interferometers. We correct for such effects using electric-field-induced waveguide nano-oxidation, demonstrating a tuning wavelength range of several nanometers and 0.002 nm resolution without line shape degradation. Field-induced nano-oxidation is a permanent and precise technique and requires no new materials or high-temperature processing.   © 2011 Optical Society of America

OCIS codes: 230.0230, 130.3120, 230.4000, 220.4241.

Silicon photonic chips consisting of dozens or hundreds of components may revolutionize short-range interconnects by achieving an essentially low power budget per bit at high bit rates, compared to copper wires [1]. In such devices, all resonant or interferometric components must be precisely aligned to a wavelength grid, or to each other. However, silicon resonators and interferometers are intrinsically highly sensitive to nanoscale fabrication disorder [2], resulting in resonant frequency shifting in microring resonators, degraded out-of-band rejection of interferometric filters, aliasing errors in arrayed waveguide gratings, and biasing errors in Mach–Zehnder modulators, and may cause localization of light [3–5]. For instance, the resonant peak may shift by as much as several hundred gigahertz for a microring resonator due to waveguide width or height variations of a few nanometers.

Various trimming and tuning techniques have been studied to compensate disorder effects in photonic devices. In particular, thermal strategies have been investigated extensively, such as microheaters placed over each component [6–8] and laser-pumped thermal tuning [9]. However, microheaters consume most of the interconnect power budget and add complexity and inefficiency to the design and layout. Other alternative methods, including atomic layer deposition [10], surface encapsulation [11], and repeated removal of native oxide using an acid etch dip [12], cannot be easily adapted to address different parts of a chip to different extents, which is necessary to combat nanoscale random disorder.

Here we demonstrate a nano-oxidation technology using an electrically biased atomic force microscope (AFM) tip at room temperature to trim silicon microrings and interferometers with high resolution and wide range. Electric-field-induced oxidation is a part of the larger class of scanning probe lithographic methods [13,14], used, e.g., to create nanoelectronic devices [15] and tune III–V photonic crystals [16], and can be parallelized for multicomponent structures [17]. For a silicon photonic device, we use this field-induced technology to locally change the waveguide core material, silicon ($n = 3.48$ at $\lambda = 1550$ nm), into the cladding material, silicon dioxide ($n = 1.44$ at $\lambda = 1550$ nm). No other new material, other than what is already used in CMOS-compatible fab-

rication, is introduced, and the field-induced oxidation, unlike thermal oxidation [18], can be performed at room temperature, which is an important consideration for doped structures, e.g., ring or Mach–Zehnder interferometric modulators. The lateral resolution achieved is less than 100 nm, which is determined by the extent of the water column formed near the tip apex, and different devices on the same chip can be trimmed individually with no crosstalk.

Field-induced oxidation occurs in ambient conditions by the spontaneous formation of a nanometer-sized water column under the metallic AFM tip. The consumption of silicon from the waveguide height decreases the effective modal refractive index, and the corresponding growth of the oxide increases the index slightly (compared to an air-clad waveguide). The volume expansion ratio for the grown oxide relative to silicon is between 2 and 3, depending on the experimental conditions, and is higher than that of thermally grown oxide. However, the propagating light in the silicon waveguide cannot distinguish between the different compositions of a few nanometers of oxide grown using field-induced oxidation and the few microns of deposited oxide conventionally used as the waveguide cladding. The net observed effect is a blueshift in the spectrum of an oxidized microring resonator, contrary to the redshift caused by thermal heating of silicon rings. In our experiments, we used a modified commercial AFM with a Pt tip (length $300\,\mu m$, force constant $20\,\mathrm{Nm^{-1}}$, tip apex radius <20 nm) for oxidation.

We have tuned both a feedback (microring resonator) and a feed-forward (Mach–Zehnder interferometer) device, as shown in Figs. 1 and 2. Devices were fabricated in house via electron-beam lithography and reactive-ion etching (RIE). The silicon-on-insulator wafer comprised a 250 nm silicon layer on top of a $3\,\mu m$ thick buried oxide. An etch depth of 160 nm was deployed to form the ridge waveguide geometry, and the waveguide width was $0.5\,\mu m$. Typically, a $9\,\mu m$ long segment of the waveguide was scanned with a 10 V tip voltage relative to the sample surface and a tip speed of $3\,\mu m^2/s$ (the net time needed for scanning over a $9\,\mu m$ segment, therefore, would be 1.5 s). Up to 100 successive oxidation scans were performed at one site before the tip was moved to a new site,
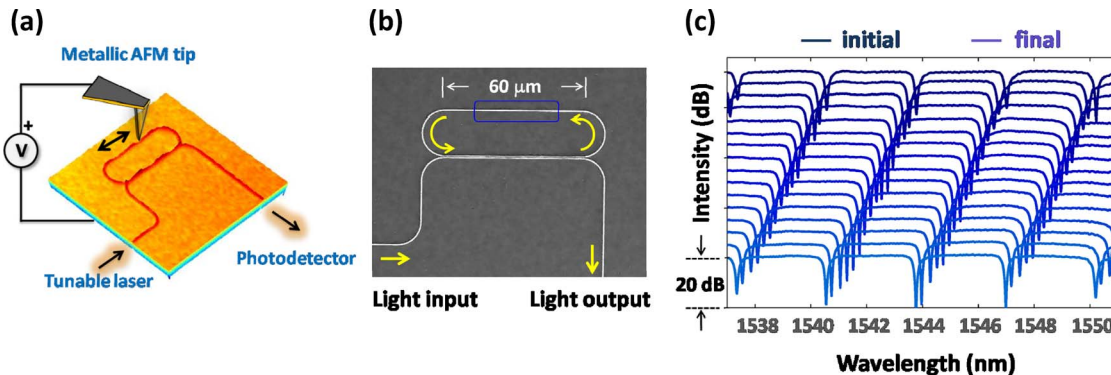
Fig. 1. (Color online) Tuning a microring resonator (MRR). (a) Schematic of electrically induced oxidation of a section of the microring. (b) Scanning electron microscope (SEM) image of a silicon MRR, with the light path indicated by yellow arrows and the oxidized region by the blue rectangle. The upper arm of the racetrack microring was progressively oxidized by scanning over $9\,\mu m$ segments with an applied voltage of $+10\,V$ at $26\,°C$, 27% relative humidity. (c) Measurements of the intensity transmission at intervals of 25 oxidation scans showed that the resonance was shifted toward shorter wavelengths (blueshifted) over its full free spectral range ($>3.1\,nm$) while preserving sharp resonances ($>15\,dB$ extinction) and no line shape deformation.

in order to avoid saturation (the oxide growth rate depends on the thickness of oxide that has already been grown [19]). No degradation of the spectra was observed.

Trimming over the complete free spectral range ($3.1\,nm$ for the microring and $12\,nm$ for the Mach–Zehnder interferometer) was achieved without peak degradation
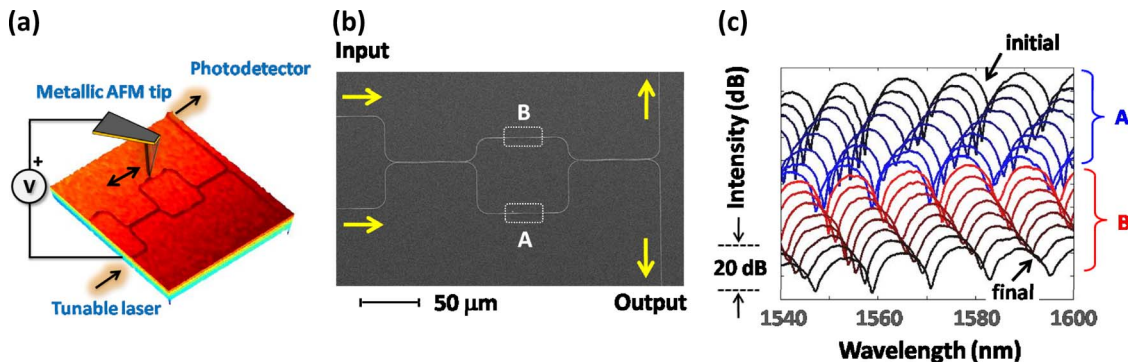

Fig. 2. (Color online) Tuning of a Mach–Zehnder interferometer (MZI). (a) Schematic of oxidation of a section of the interferometer. (b) SEM image of an MZI that serves as a 2×2 routing gate (crossbar switch architecture), with regions to be oxidized indicated as A and B. (c) Measurements of the intensity transmission (shown at intervals of 50 oxidation scans) indicated that the transmission peaks and valleys were systematically shifted to shorter wavelengths (blueshifted) as a consequence of oxidizing region B, then back to longer wavelengths (redshifted) when region A was oxidized. Tunability over the full free spectral range ($12\,nm$) was achieved; thus the MZI can be programmed to any desired transmission over the entire $60\,nm$ range of wavelengths.
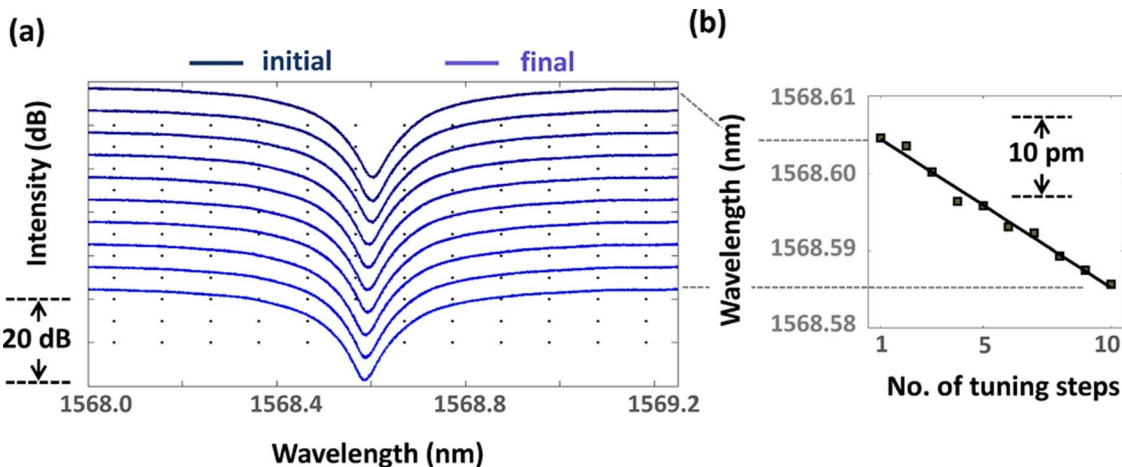

Fig. 3. (Color online) Resolution of tuning. (a) A silicon MRR was tuned in single-scan oxidation steps for very accurate resonance positioning over a narrow range of wavelengths while preserving high-contrast extinction ratio ($>20\,dB$). Rows of dots indicate the most stringent International Telecommunications Union (ITU-T) G.941.1 spectral grid spacing (for 12.5 GHz carrier-class telecommunications systems). (b) The resonance wavelengths blueshifted linearly with a slope of $-2.1\,pm$ (approximately $260\,MHz$)/scan.

(>15 dB extinction) or line shape deformation. For the Mach–Zehnder interferometer, bidirectional trimming is possible, depending on which arm the oxidation was performed; thus, an interferometric null (or, alternatively, a peak or a midpoint) could be achieved at any target wavelength within a wide 60 nm span of wavelengths.

Very-high-resolution trimming of a silicon microring resonator is shown in Fig. 3, by reducing the oxidized segment length to $0.5\,\mu m$. The change of the modal effective index can be calculated from the length of the waveguide that is oxidized L_{ox} ($0.5\,\mu m$), the round-trip racetrack length L_{rt} ($183\,\mu m$), the measured wavelength shift of a single scan [260 MHz; see Fig. 3(b)], the modal effective index ($n_{eff} = 2.63$ at $\lambda = 1.55\,\mu m$), and its dispersion,

$$\Delta n_{eff} = -\frac{L_{rt}}{L_{ox}}\left(\frac{\Delta\lambda}{\lambda}\right)n_{eff}(\lambda)\left(1 - \frac{\lambda}{n_{eff}(\lambda)}\frac{dn_{eff}}{d\lambda}\bigg|_{\lambda}\right), \quad (1)$$

where the second (dispersive) term inside the parentheses is significant and evaluates to 0.525 at $\lambda = 1.55\,\mu m$ for the fabricated waveguides. Thus, an effective index change of -7.53×10^{-4} was calculated. Based on modeling of the transverse cross section of the waveguide in a finite-element mode solver (COMSOL), an effective silicon consumption rate of $1.6\,\text{Å/scan}$ was inferred, consistent with earlier reports [19]. Further reduction of the area of oxidation region based on lateral resolution, increasing the tip–sample distance, lowering the bias voltage, or changing the humidity and temperature might lead to a smaller trimming resolution limit.

In summary, our results demonstrate field-induced nano-oxidation trimming of silicon waveguides as a site-specific, precise, controllable, and permanent method for compensating for spectral misalignment that arises from nanoscale disorder in today's silicon photonic devices. After trimming, no further energy consumption is necessary in order to "hold" the final state, unlike with micro-heaters, and therefore, field-induced oxidation may be useful for realizing energy-efficient and high-performance silicon photonic circuits that consist of multiple resonators and interferometers.

References

1. P. K. Pepeljugoski, J. A. Kash, F. Doany, D. M. Kuchta, L. Schares, C. Schow, M. Taubenblatt, B. J. Offrein, and A. Benner, in *Optical Fiber Communication Conference*, OSA Technical Digest (CD) (Optical Society of America, 2010), paper OThX2.
2. W. A. Zortman, D. C. Trotter, and M. R. Watts, Opt. Express **18**, 23598 (2010).
3. T. Barwicz, H. Byun, F. Gan, C. W. Holzwarth, M. A. Popovic, P. T. Rakich, M. R. Watts, E. P. Ippen, F. X. Kartner, H. I. Smith, J. S. Orcutt, R. J. Ram, V. Stojanovic, O. O. Olubuyide, J. L. Hoyt, S. Spector, M. Geis, M. Grein, T. Lyszczarz, and J. U. Yoon, J. Opt. Netw. **6**, 63 (2007).
4. F. Xia, L. Sekaric, and Y. Vlasov, Nat. Photon. **1**, 65 (2007).
5. S. Mookherjea, J. S. Park, S.-H. Yang, and P. R. Bandaru, Nat. Photon. **2**, 90 (2008).
6. C. T. DeRose, M. R. Watts, D. C. Trotter, D. L. Luck, G. N. Nielson, and R. W. Young, in *Conference on Lasers and Electro-Optics*, OSA Technical Digest (CD) (Optical Society of America, 2010), paper CThJ3.
7. P. Dong, W. Qian, H. Liang, R. Shafiiha, D. Z. Feng, G. L. Li, J. E. Cunningham, A. V. Krishnamoorthy, and M. Asghari, Opt. Express **18**, 20298 (2010).
8. A. Faraon and J. Vučković, Appl. Phys. Lett. **95**, 043102 (2009).
9. J. Pan, Y. Huo, K. Yamanaka, S. Sandhu, L. Scaccabarozzi, R. Timp, M. L. Povinelli, S. Fan, M. M. Fejer, and J. S. Harris, Appl. Phys. Lett. **92**, 103114 (2008).
10. C. J. Chen, C. A. Husko, I. Meric, K. L. Shepard, C. W. Wong, W. M. J. Green, Y. A. Vlasov, and S. Assefa, Appl. Phys. Lett. **96**, 081107 (2010).
11. M. Borselli, T. J. Johnson, C. P. Michael, M. D. Henry, and O. Painter, Appl. Phys. Lett. **91**, 131117 (2007).
12. A. Badolato, Science **308**, 1158 (2005).
13. J. A. Dagata, J. Schneir, H. H. Harary, C. J. Evans, M. T. Postek, and J. Bennett, Appl. Phys. Lett. **56**, 2001 (1990).
14. I. W. Lyo and P. Avouris, Science **253**, 173 (1991).
15. C. Cen, S. Thiel, J. Mannhart, and J. Levy, Science **323**, 1026 (2009).
16. K. Hennessy, C. Högerle, E. Hu, A. Badolato, and A. Imamoğlu, Appl. Phys. Lett. **89**, 041118 (2006).
17. J. Martinez, N. S. Losilla, F. Biscarini, G. Schmidt, T. Borzenko, L. W. Molenkamp, and R. Garcia, Rev. Sci. Instrum. **77**, 086106 (2006).
18. J. Zheng, C. J. Chen, J. F. McMillan, M. Yu, G.-Q. Lo, D.-L. Kwong, and C. W. Wong, in *CLEO:2011—Laser Applications to Photonic Applications*, OSA Technical Digest (CD) (Optical Society of America, 2011), paper AMA3.
19. P. Avouris, R. Martel, T. Hertel, and R. Sandstrom, Appl. Phys. A **66**, S659 (1998).